

Seismic Performance Assessment of Concentrically Braced Steel Frame Buildings

Chui-Hsin Chen¹, Jiun-Wei Lai¹ and Stephen Mahin²

¹ Graduate Student, Dept. of Civil and Env. Eng., Univ. of Calif., Berkeley, CA, USA

² Professor, Dept. of Civil and Env. Eng., Univ. of Calif., Berkeley, CA, USA

Email: chchen@berkeley.edu, adrian.jwlai@berkeley.edu, mahin@berkeley.edu

ABSTRACT:

Three-story tall, model building systems are analyzed using OpenSEES to improve understanding of the behavior of conventionally braced and buckling restrained braced frames, and to identify improved performance-based design and analysis procedures. The analyses demonstrate that statistically, the three-story model building designed following 1997 NEHRP and that following ASCE 7-05 have similar performance in terms of the damage concentration. If the R value is reduced from 6 to 3, the demands on the braces and framing components are reduced as well as the tendency to form a soft story. However, stronger structure results in higher floor level accelerations, possibly creating greater falling hazards or increasing the costs of protecting nonstructural components and hazards. For the three-story BRBF model the tendency to form a soft story is less than SCBF. Nonetheless, the BRBF model has the largest residual drifts. A preliminary examination of floor level accelerations shows that the peak accelerations appear to be limited by the strength of the structure. The testing protocols are evaluated based on the analytical results, but further experiments are needed to verify the results. Based on the parametric study, four large-scale two-story braced frames with different brace types and different bracing configurations are designed to be tested in the University of California at Berkeley. Test results will be used to refine the analytical models and validate the seismic performance of SCBF and BRBF.

KEYWORDS: Performance-based design, Special Concentrically Braced Frame, Buckling Restrained Braced Frame

1. INTRODUCTION

A series of nonlinear dynamic analyses are presented that extend earlier work by Uriz (2005). In addition to updating the building code used, the configuration of the structure is altered from a stacked chevron arrangement to one where the braces are arranged in a double story X configuration.

The model buildings are three-story tall SCBF and BRBF structures. A variety of results are presented to assess likely behavior for different seismic hazard levels in terms of peak roof displacement, interstory drifts, residual story displacements, and floor level accelerations.

2. DESIGN CRITERIA

This study is confined to an assessment of the seismic response of two nearly identical three-story tall steel buildings. As seen in Figure 1, the model buildings have regularly spaced gravity-resisting frames (continuous columns with ideal pin connections to the beams and foundation) with lateral earthquake-load resistance provided by special concentric braced frames (SCBF) or buckling restrained braced frames (BRBF) located on the perimeter of the building. These buildings were designed by others [Sabelli 2000, DASSE 2007] for a location in downtown Los Angeles, CA as commercial office buildings (Occupancy Category II). One of the model buildings was designed in conformance with the provisions of the 1997 NEHRP seismic design provisions and the others were designed in conformance with the provisions of ASCE 7-05. The importance factor and redundancy factor were assumed to be unity for all designs. Table 1 lists some of the principal attributes of the structures and the key parameters used in the seismic design.

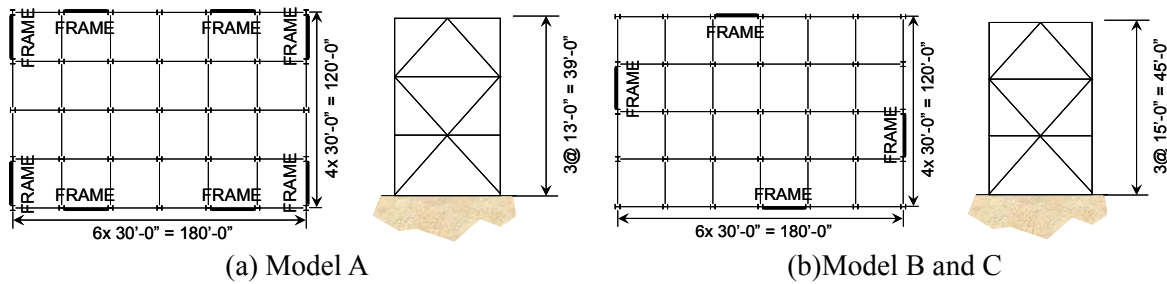


Figure 1 Model building floor plan and elevation

Table 1 Design parameters of model buildings

Code	1997 NEHRP	ASCE 7-05
Short Period Spectral Acceleration, S_s	2.09g	2.20g
1 sec. Period Spectral Acceleration, S_1	0.77g	0.74g
F_a	1.0	1.0
F_v	1.5	1.5
R	6	6 (SCBF), 8 (BRBF)
Design Base Shear	0.23W	0.24W (SCBF), 0.13W (BRBF)

3. MODEL BUILDINGS

Table 2 lists the member sizes used in the models. Model A represents the typical SCBF bent designed based on 1997 NEHRP provisions, while model B and C represent SCBF and BRBF systems designed based on ASCE 7-05. The configuration of lateral load-resisting frames are also different, with model A having twice as many lateral load resisting bents. The story height for model A is 13 feet, whereas that for model B and C is 15 feet.

The roof beam of model A is particularly light comparing to the lower two floor beams, because the 1997 AISC Seismic Provisions contain an exception to the normal strong beam design requirement at the roof of chevron SCBF systems. In model B, because the unbalanced loads induced from the buckling of braces on the top story are considered in the 2005 AISC Seismic Provisions, the roof beam is considerably heavier than the 2nd and 3rd floor girders. In model C, the member sizes are typically smaller because of the greater R value, the reduced brace unbalanced forces, and the longer fundamental period and therefore smaller design acceleration.

Table 2 Member sizes

Structural Element	Model	2 nd	3 rd	Roof
Braced Frame Columns	A	W12x96	W12x96	W12x96
	B	W14x176	W14x176	W14x176
	C	W14x132	W14x132	W14x132
Braced Frame Beams	A	W30x90	W27x84	W18x46
	B	W27x84	W30x116	W36x210
	C	W24x76	W24x76	W24x76
Brace Size	A	HSS 8x8x1/2	HSS 8x8x1/2	HSS 6x6x3/8
	B	HSS 10.0x0.375	HSS 11.25x0.50	HSS 12.5x0.50
	C	7.5 in ²	6 in ²	4 in ²

4. OPENSEES NUMERICAL MODELS

Four model buildings, designated 3AF, 3BF, 3BF₃, 3CF, were analyzed using the computational framework OpenSees [McKenna 1997]. The notation used for the model names is listed in Table 3. The beams were considered to be rigidly connected to the columns in all models. Two variations of model B were compared in this paper. Model 3BF had rigid connections of the beams to the columns. Model 3BF₃ was similar to model 3BF, except twice as many braced bents were used. Thus, a force reduction factor R of 3 (rather than 6) was

effectively used for model 3BF₃. Model 3CF was also similar to model 3BF except for using buckling restrained braces. Rigid end zones are considered in all the models, as illustrated in Figure 2, to represent the physical size and stiffening effect of the gusset plates. The vertical floor mass tributary to the brace was modeled [Khatib et al. 1988]. Also considered in all of the models was a simplified “leaning” column with pin on each floor level to account for P-Δ effects.

The braces including the gusset plates in the ends were modeled with force-based nonlinear beam-column element. Fiber sections were used for the critical sections where yielding might occur. The beam and columns were modeled similarly to capture inelastic behavior. A corotational formulation was used to model member buckling while local buckling was not explicitly modeled. An empirical cycle counting method was used to simulate rupture due to low-cycle fatigue [Uriz 2005].

Table 3 Model names

Abbreviation	Denotation
A	Double story X SCBF designed to comply with 1997 NEHRP
B	Double story X SCBF designed to comply with ASCE 7-05
C	Double story X BRBF designed to comply with ASCE 7-05
F	Model building with fully constrained beam-column connections
Subscript 3	Model building designed with R=3 instead of R=6 for SCBF

5. DESIGN SPECTRA

The seismic spectra considered in the design of the three model buildings are shown in Figure 3. The spectra are quite similar, though in the constant amplified acceleration range, the ASCE 7-05 spectra is slightly larger than that in the 1997 NEHRP provisions.

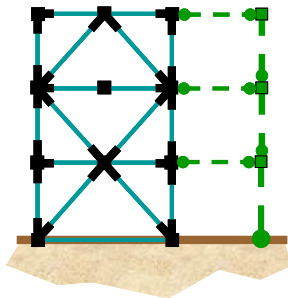


Figure 2 Sketch of basic OpenSEES model

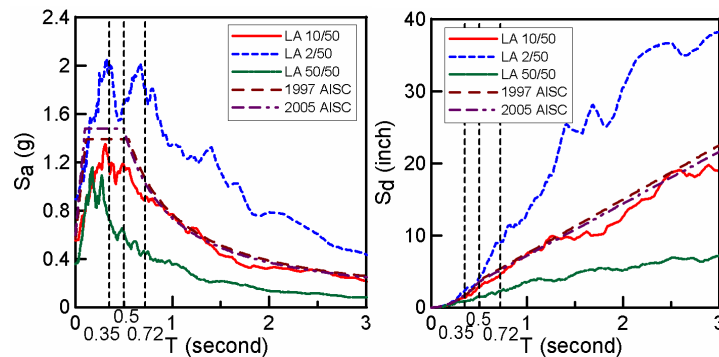


Figure 3 Response spectra

Sixty ground motion records were used to conduct nonlinear dynamic analysis of each of the four models. These records were taken from the SAC ground motion ensembles developed consistent with the 1997 NEHRP seismic hazard curves for Los Angeles [Somerville 1997]. The sixty records represent three hazard levels (10% probability of exceedence in 50 years, 2% in 50 years and 50% in 50 years). The median of the pseudo-spectral acceleration and spectral displacement of the 20 ground motion records corresponding to a particular hazard level are shown in Figure 3. The median elastic spectral displacements corresponding to the fundamental period of the various models is shown in Table 4 for the three hazard levels considered.

Table 4 Median of $S_{d,Elastic}$ (inch)

Model	Hazard Level		
	50% in 50yrs	10% in 50yrs	2% in 50yrs
3AF, T=0.36 sec.	1.12	1.63	2.44
3BF, T=0.49 sec	1.70	2.74	4.13
3BF ₃ , T=0.35 sec.	1.07	1.56	2.30
3CF, T=0.72 sec.	2.86	4.67	9.31

6. STATISTICAL EVALUATION FROM ANALYSES

The statistical variation of various engineering demand parameters are examined for the sixty SAC ground motions recorded.

6.1 Interstory Drift Demands

Figures 4 to 6 shows the relation of peak interstory drift ratio to $S_{d,Elastic}$. $S_{d,Elastic}$ is taken as the elastic spectral displacement for the record used in the analysis at the fundamental period of the model being simulated. In the plot, IDRAve is the peak roof displacement divided by the total height of the model building (which is thus the average interstory drift ratio); IDRmax is the maximum interstory drift ratio occurring at any of the three stories. The ratio of IDRmax/IDRAve can be regarded as the index of the tendency to form a soft story. The higher the ratio, the more concentrated the damage is in a single story. Linear regression analyses have been performed considering all of the results for a particular model, to obtain relations of the form $\ln IDR = b + m \cdot \ln S_{d,Elastic}$.

Comparing model 3AF and 3BF in Figure 4 and accounting for the difference in the fundamental periods of the various models, the drifts of 3BF are slightly higher but the tendency to concentrate damage is similar for the two models. The IDRmax/IDRAve ratio in Table 5 also demonstrates the observation.

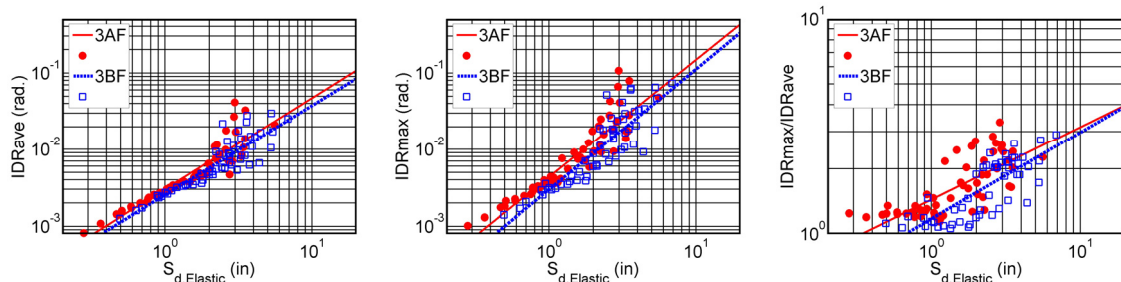


Figure 4 Interstory drift ratio for different design codes

Table 5 Median expected engineering demand parameters corresponding to different hazard levels

Model Hazard Level	3AF			3BF			3BF ₃			3CF		
	50/50	10/50	2/50	50/50	10/50	2/50	50/50	10/50	2/50	50/50	10/50	2/50
IDRmax (radian)	0.52%	0.92%	1.71%	0.69%	1.46%	2.78%	0.33%	0.55%	0.91%	1.08%	1.80%	3.68%
IDRAve (radian)	0.35%	0.54%	0.88%	0.47%	0.83%	1.34%	0.27%	0.40%	0.60%	0.78%	1.27%	2.55%
IDRmax/IDRAve	1.50	1.70	1.95	1.45	1.76	2.08	1.22	1.36	1.53	1.40	1.42	1.44
Res. IDR (rad.)	0.03%	0.09%	0.30%	0.06%	0.22%	0.65%	0.01%	0.03%	0.11%	0.16%	0.34%	0.98%

Model 3BF₃ is twice as stiff and strong as model 3BF. Thus, similar to model 3AF, the fundamental period and $S_{d,Elastic}$ values for model 3BF₃ are significantly less than those for model 3BF. The trend lines in Figure 5 show that the average and maximum IDRs are usually smaller for model 3BF₃ than for model 3BF for the same value of $S_{d,Elastic}$. In IDRmax/IDRAve plot, model 3BF₃ tends to have smaller ratio if $S_{d,Elastic}$ is the same, but since model 3BF₃ has a smaller $S_{d,Elastic}$ value, the tendency to form a soft story is actually further reduced. The index is listed in Table 5.

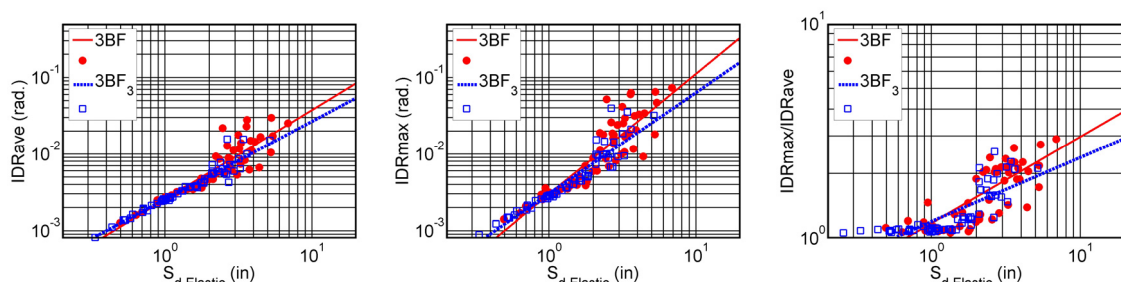


Figure 5 Interstory drift ratio for R=6 and R=3

Comparing models 3BF and 3CF, the regression line of average IDRs for both models are rather similar (Figure 6). Considering the difference of $S_{d,Elastic}$, the maximum IDR is greater than that of model 3BF (see Table 5). The BRBF tends to spread the IDR out through the whole building, since the braces do not buckle and deteriorate. The tendency to form a soft story is much less than SCBF as seen in Figure 6.

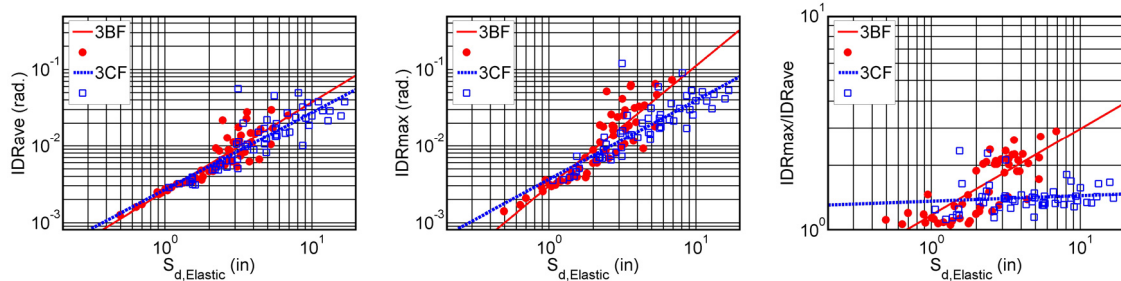


Figure 6 Interstory drift ratio for three-story, double-story X SCBF and BRBF

Figure 7 demonstrates the probability that the maximum interstory drift ratio will exceed 0.3% and 2.5% radians. The interstory drift ratio at first buckling of a brace is about 0.3%. Considering the 50% in 50-year hazard level, models 3AF, 3BF and 3BF₃ have 69.3, 78.5 and 38.6% probabilities of buckling a brace at one or more levels. This points out the need to consider likely local nonstructural damage during service level events, and the possible need to replace braces following such events due to permanent lateral offsets. Considering the 2% in 50 years hazard level, the same models have 85.0, 93.4 and 74.7% probabilities of exceeding 2.5% drift.

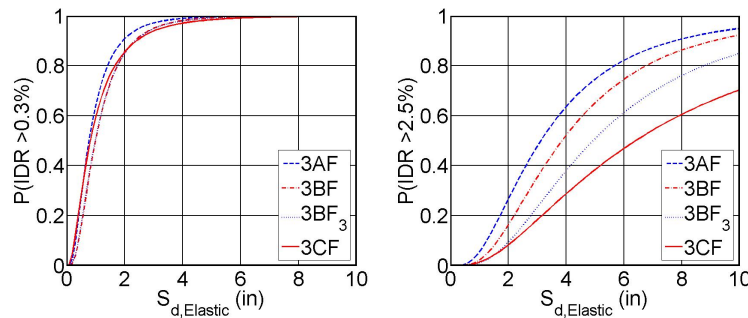
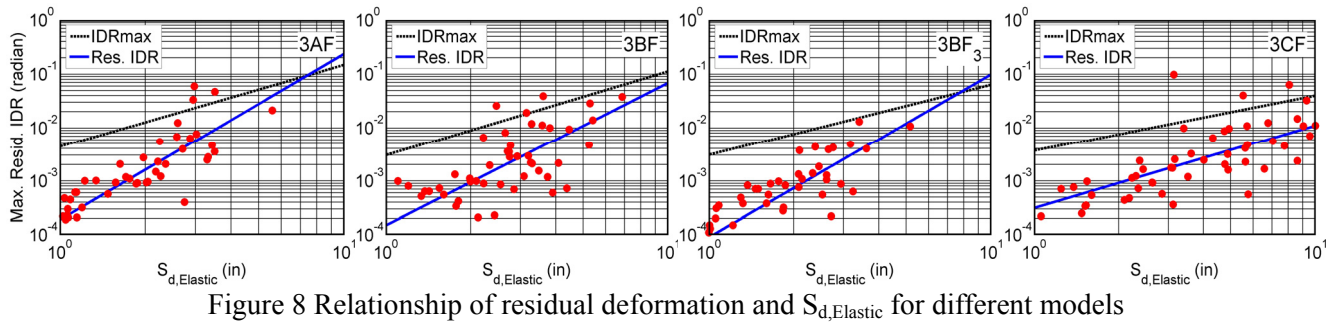


Figure 7 Probability of exceeding critical drift for different models

6.2 Residual Interstory Drift Demands

Residual displacement is a key determinant in whether it is feasible to repair a structure following an earthquake. The residual interstory drift ratios of each model corresponding to different hazard levels are listed in Table 5. Figure 8 presents the relation of the maximum residual interstory drift remaining at the end of the earthquake and $S_{d,Elastic}$. Two lines are superimposed, where one represents the median linear regression analysis result for the residual interstory drift ratio, whereas the other represents the previously reported maximum interstory drift ratio. It is clear that there is tremendous scatter in the peak interstory residual displacements. In some cases, the residual displacement significantly exceeds the median expected maximum displacement at a particular value of $S_{d,Elastic}$, while in other cases the residual displacement is quite small.

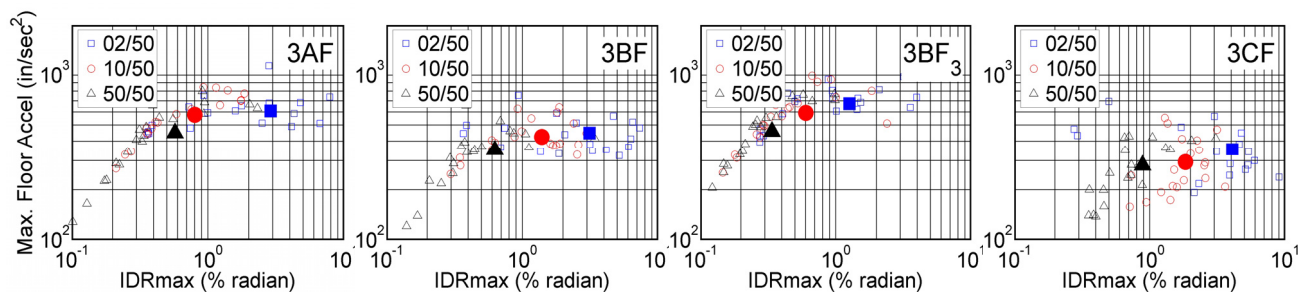
The trend for residual displacements is such that the residual drifts become a larger fraction of the maximum drifts as the intensity of shaking increases. This is less pronounced in model 3CF, because the regression lines in Figure 8 are more parallel. Also, model 3CF tends to have larger residual displacement than the other models partly because of the longer fundamental period and partly because of the properties of the buckling restrained braced frames.



6.3 Floor Level Acceleration Demands

Life safety hazards can develop as a result of falling objects. The potential for nonstructural elements and contents falling is related to floor level accelerations. In addition to posing a life safety hazard, acceleration sensitive objects can be dislodged or damaged, requiring considerable effort and funds to repair following an earthquake. As such, the assessment of the maximum peak floor level accelerations has been carried out.

Instead of presenting this information in a manner similar to Figures 4 to 6, the computed maximum interstory drifts and floor level accelerations for each record are plotted for each model in Figure 9. The computed demands appear as clouds of points, with the 2% in 50 year hazard level events represented by hollow squares, the 10% in 50 year events represented by hollow circles, and the 50% in 50 year events represented by hollow triangles. The center of gravity of these points are represented by a solid square, circle and triangle. From this plot, it can be seen that the displacements increase with increasing hazard level (ground motion intensity), but the maximum accelerations do not increase as dramatically. The accelerations for model 3AF and 3BF₃ show consistently higher accelerations than model 3BF. This may be explained by the higher strength and stiffness of model 3AF and 3BF₃. For model 3CF, because of the relatively longer fundamental period, the maximum IDR is greater while the maximum floor accelerations are smaller than other models.



7. EVALUATION OF TESTING PROTOCOLS

With the analytical results, the testing protocol for SCBF can be studied from the point of view of the statistics. The procedure to evaluate the testing protocol follows previous studies [Krawinkler 2000 et al.]. The IDR range which dominates the failure criteria was extracted from the analytical results of model 3BF. Only the most severe hazard level was investigated including the responses of SCBF to 20 ground motions corresponding to a 2% in 50 year hazard level. The cumulative density function is given in Figure 10 and several testing protocols are compared. The CDF curve for the SCBFs is usually steeper than for MRFs in the small IDR range because more small cycles occur in the SCBFs. Also, the CDF of the SCBFs is usually greater in a smaller IDR ranges comparing to the MRFs. The step function of the protocol in SAC MRF reflects this observation. The protocol in FEMA 461, which is for general use for all kind of structural and nonstructural components, has the trend close to SAC MRF. The trial protocol proposed here, adopts the protocol similar to SAC MRF and calibrated by the CDF from the analytical results of SCBFs (model 3BF). The step function of trial protocol is relatively

closer to the statistical results than other protocols. Nonetheless, more experimental studies may be of great help for the further investigations.

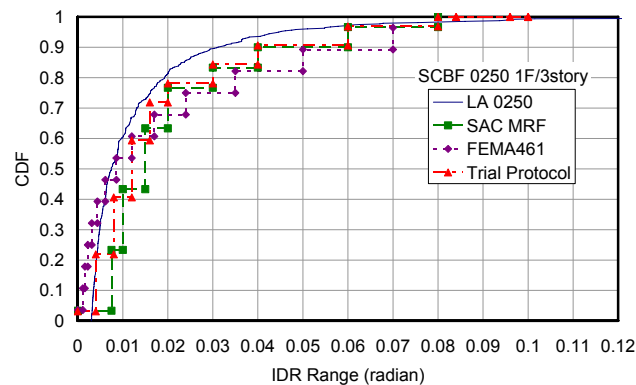


Figure 10 Matching of testing protocols with CDF of three-story SCBF in 2/50 hazard level

8. ON-GOING EXPERIMENTS

A series of testing on large-scale two-story braced frames is underway. Figure 11 illustrates the test setup of the experiments at UC, Berkeley. Specimens include two SCBFs and two BRBFs with different design parameters, such as brace configurations, brace b/t ratio, brace KL/r ratio and connection details. The initial stage is to test the diamond shape conventional braced frame as illustrated in Figure 12. In addition to the global behavior, the beam-column-brace connection is one of the primary variables studied. The further testing specimens will be designed upon the first experimental results.

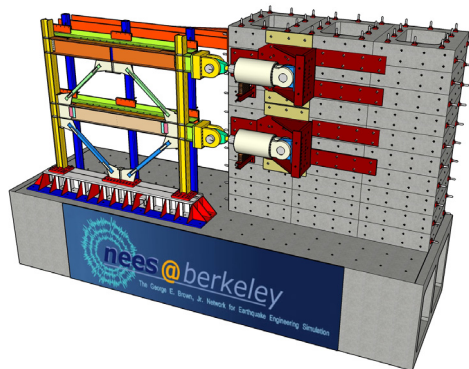


Figure 12 Tentative test setup

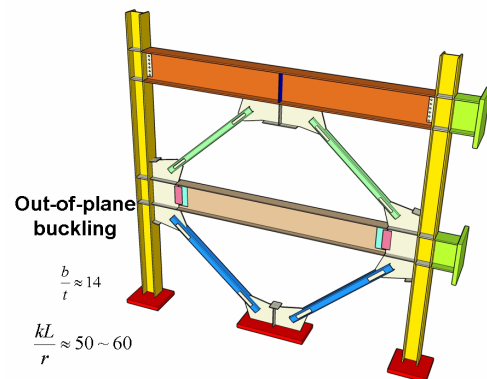


Figure 13 Test specimen

9. CONCLUSION

The analytical study of SCBF buildings was conducted using OpenSEES. The systems are characterized by a tendency to concentrate damage in a few stories. According to the analyses, the performance of SCBF designed as per ASCE7-05 and 1997 NEHRP are quite similar. If the R value is reduced from 6 to 3, the tendency to form a soft story can be reduced. As for the BRBF, the tendency to form a soft story is less than SCBF. Residual lateral drifts can be considerable for all models as the intensity of ground shaking increases. Among all the analyses, the BRBF model has the largest residual drifts. A preliminary examination of floor level accelerations shows that drifts and accelerations vary by different amounts as the intensity of shaking increases. In particular, at large levels of shaking, the peak accelerations appear to be limited by the strength of the structure.

The SCBF is stiffer than many other structural systems. As such, the general testing protocol which cannot capture the responses of small cycles maybe modified to apply to SCBFs. More experiments are required to validate the global and local responses of the SCBFs, and also to verify the adequacy of the testing protocols.

Work on this project is on going. The work is extended to consider six story SCBF and BRBF models. The experimental study is also underway. The test results will be used to modify numerical models as well as investigating the potential damages braced frames may encounter.

ACKNOWLEDGEMENTS

This work is an extension of previous work by Dr. Patxi Uriz. His assistance in developing the numerical models and providing advice is greatly appreciated. Rafael Sabelli designed the SCBF structures considered herein; his efforts to design the specimens and provide advice related to interpretation of code requirements contributed to the success of this effort. The assistance of Silvia Mazzoni in developing the OpenSEES models is gratefully acknowledged. The comparison of OpenSEES models with finite element models is underway with the efforts of Yuli Huang. His efforts is greatly acknowledged.

This material is based upon work supported in part by the National Science Foundation under Grant No. CMS-0600625 -- Robust Performance-based Design of Concentrically Braced Steel Frame Buildings, and Grant No. 0619161 -- International Hybrid Simulation of Tomorrow's Braced Frame Systems. Any opinions, findings, and conclusions or recommendations expressed in this material are those of the author(s) and do not necessarily reflect the views of the National Science Foundation.

REFERENCES

- AISC. (1997), Seismic Provisions for Structural Steel Buildings, American Institute of Steel Construction, Chicago, Illinois.
- AISC. (2005), Seismic Provisions for Structural Steel Buildings, American Institute of Steel Construction, Chicago, Illinois.
- ASCE 7 (2005), ASCE Standard Minimum Design Loads for Buildings and Other Structures, ASCE 7-05, American Society of Civil Engineers, Reston, VA.
- ATC (2007), Interim Testing Protocols for Determining the Seismic Performance Characteristics of Structural and Nonstructural Components, FEMA 461 Report, prepared by Applied Technology Council for the Federal Emergency Management Agency, Washington, D.C.
- DASSE (2007), Cost Advantages of Buckling Restrained Braced Frame Buildings, DASSE Design Inc.
- Khatib, I., Mahin, S. and Pister, K. (1988), Seismic behavior of concentrically braced steel frames, UCB/EERC-88/01, Earthquake Engineering Research Center, University of California, Berkeley, 1988-01, 222 pages
- Krawinkler, H., Gupta, A., Medina, R., and Luco, N. (2000), Loading history for seismic performance testing of SMRF components and assemblies, Sacramento, Calif.: SAC Joint Venture. (SAC/BD-00/10)
- McKenna, F. (1997). Object Oriented Finite Element Programming: Frameworks for Analysis, Algorithms and Parallel Computing, University of California, Berkeley, Berkeley, CA 94720.
- NEHRP (1997), Recommended Provisions for the Development of Seismic Regulations for New Buildings (and other Structures), Building Seismic Safety Council, Washington, D.C.
- Sabelli, R. (2000), Research on Improving the Design and Analysis of Earthquake Resistant Steel Braced Frames, FEMA / EERI.
- Somerville, P. G. (1997). Development of ground motion time histories for phase 2 of the FEMA /SAC Steel Project. *SAC BD/97-04*, SAC Steel Joint Venture, Sacramento California.
- Uriz, P (2005), Towards earthquake resistant design of concentrically braced steel structures, Ph.D. Dissertation, Department of Civil and Environmental Engineering, University of California, Berkeley, CA.